Journal Pre-proof

Mass transfer kinetics on modern Whelk-O1 chiral stationary phases made on fully- and superficially-porous particles

Simona Felletti, Martina Catani, Giulia Mazzoccanti, Chiara De Luca, Giulio Lievore, Alessandro Buratti, Luisa Pasti, Francesco Gasparrini, Alberto Cavazzini

PII: S0021-9673(20)31128-6
DOI: https://doi.org/10.1016/j.chroma.2020.461854
Reference: CHROMA 461854

To appear in: *Journal of Chromatography A*

Received date: 31 October 2020
Revised date: 22 December 2020
Accepted date: 23 December 2020

Please cite this article as: Simona Felletti, Martina Catani, Giulia Mazzoccanti, Chiara De Luca, Giulio Lievore, Alessandro Buratti, Luisa Pasti, Francesco Gasparrini, Alberto Cavazzini, Mass transfer kinetics on modern Whelk-O1 chiral stationary phases made on fully- and superficially-porous particles, *Journal of Chromatography A* (2020), doi: https://doi.org/10.1016/j.chroma.2020.461854

Highlights

- Investigation of mass transfer in chiral Whelk-O1 stationary phases
- Demonstration of localized adsorption (no surface diffusion) in this system
- Adsorption-desorption kinetics estimated by combining kinetics and thermodynamics

Mass transfer kinetics on modern Whelk-O1 chiral stationary phases made on fully- and superficially-porous particles

Simona Felletti[a], Martina Catani[a], Giulia Mazzoccanti[b], Chiara De Luca[a], Giulio Lievore[a], Alessandro Buratti[a], Luisa Pasti[a], Francesco Gasparrini[b,*], Alberto Cavazzini[a,**]

[a]*Dept. of Chemistry and Pharmaceutical Sciences, University of Ferrara, via L. Borsari 46, 44121 Ferrara, Italy*
[b]*Dept. of Drug Chemistry and Technology, Sapienza Universita di Roma, P.le A. Moro 5, 00185 Roma, Italy*

Abstract

In this work, a detailed study of mass transfer properties of *trans*-stilbene oxide (TSO) enantiomers on two Whelk-O1 chiral stationary phases (CSPs) has been performed. The CSPs were prepared by using both fully-porous silica particles of 2.5 μm particle diameter and superficially-porous ones of 2.6 μm particle diameter as base materials. By combining stop-flow and dynamic measurements in normal-phase conditions, the different contributions to mass transfer have been estimated. The study of intra-particle diffusion has revealed that the adsorption of both enantiomers is localized (i.e., characterized by absence of surface diffusion). The determination of thermodynamic binding constants (measured through adsorption isotherms) supports this finding.

Keywords: Chiral chromatography, Fully- and superficially-porous particles, Mass transfer, Localized adsorption, Adsorption-desorption kinetics

1. Introduction

In the last years, the interest towards ultrafast chiral separations has significantly grown. The rapid development of chiral stationary phases (CSPs) based on silica particles suitable for high efficient separations, either sub-2μm or pellicular particles, has pushed the innovation [1–11]. So-called ultrafast chiral separations (usually this term refers to separations achieved in the order of seconds [1, 6, 12]), which only a few years ago would have been unimaginable, have been performed thanks to the combination of short columns (0.5-2 cm) and high flow-rates (5-8 ml/min). Noticeably, the enantioresolution of these systems was very large even at the highest flow-rates, at the point that the bottleneck to the attainment of even more sensational results has been the well-known pressure/flow-rate trade-off, even by using modern UHPLC equipment. Despite the achievement of these milestones, only a few studies aimed at investigating the fundamentals of mass transfer in chiral LC have been attempted [13, 14].
From a fundamental viewpoint, an intrinsic complication in chiral chromatography comes from the fact that the contribution to mass transfer coming from adsorption-desorption kinetics is very difficult to quantify. On the other hand, it is widely acknowledged that this is very often the main source of band broadening even at low flow rates and even for small molecules [15–20]. The main difference between chiral and achiral separations is indeed in the impact of adsorption-desorption kinetics on efficiency. In achiral chromatography, the adsorption-desorption kinetics are usually negligible, unless very large molecules are considered [16, 21].
From a molecular perspective, the slow adsorption-desorption kinetics in chiral chromatography finds an explanation in the fact that a specific spatial orientation of molecules is needed to establish the diastereomeric transient complexes between enantiomers and the chiral selector. This is achieved through the simultaneous onset of multiple intermolecular interactions (including steric hindrance effects and induced-fitting chiral recognition mechanisms), which often takes time.
Traditionally, in the van Deemter equation, an independent, linear contribution to the plate height accounts for the adsorption-desorption kinetics. In reduced coordinates, for chiral separations, indeed the

*Corresponding author, email: francesco.gasparrini@uniroma1.it
**Corresponding author, phone: email: cvz@unife.it, +39 0532 455389, fax: +39 0532 240709

van Deemter equation is written as:

$$h = a(\nu) + \frac{b}{\nu} + (c_s + c_{ads})\nu \quad (1)$$

with h and ν being the reduced plate-height and the interstitial velocity, respectively, $a(\nu)$ a complex function of reduced flow velocity describing the eddy dispersion, b the longitudinal diffusion, c_s the mass transfer resistance across the stationary phase [16] and, finally, c_{ads} the adsorption-desorption kinetics.

If c_{ads} is negligible (e.g., achiral separations of small molecules), all contributions to mass transfer can be singled out since b and c_s can be independently estimated through stop-flow measurements (and a proper model of diffusion through porous materials) [16, 22]. Indeed, the eddy dispersion can be estimated by simply subtracting b and c_s from h (see Eq. 1, with $c_{ads} = 0$). On the opposite, in chiral chromatography, this approach leads to the sum of eddy dispersion and adsorption-desorption terms:

$$h - \frac{b}{\nu} - c_s\nu = a(\nu) + c_{ads}\nu \quad (2)$$

In this paper, two Whelk-O1 CSPs were prepared on superficially porous particles (SPPs) of 2.6 μm particle diameter and fully porous particles (FPPs) of 2.5 μm particle diameter. The particles were packed into stainless steel columns. These columns were fully characterized through peak parking experiments and van Deemter curves by using *trans*-stilbene oxide (TSO) enantiomers as probes. Finally, a semi-empirical approach has been suggested to overcome the intrinsic problem of Eq. 2 and to estimate the impact of adsorption-desorption kinetics. To this end, results of the investigation were cross-referenced with thermodynamic data (from adsorption isotherms) obtained in a previous work for the same probes and experimental conditions [23].

2. Experimental Section

2.1. Columns and materials

All solvents and reagents were purchased from Merck (Darmstadt, Germany), so were TSO enantiomers. Kromasil silica (2.5 μm particle size, 100 Å pore size, 323 m^2/g specific surface area) was from Akzo-Nobel (Bohus, Sweden). Accucore silica (2.6 μm, 80 Å, 130 m^2/g, ρ = 0.63) was from Thermo Fisher Scientific (Waltham, MA, USA). Whelk-O1 selector was generously donated by Regis Technologies Inc. (Morton Grove, IL, USA). 150 mm×4.6 mm empty stainless steel columns were from IsoBar Systems by Idex (Erlangen, Germany). Synthesis and preparation of Whelk-O1 CSPs are reported in Ref. [1]. A 33 ×4.6 mm Micra column (Eprogen, Inc., USA) packed with 1.5 μm non-porous silica particles was purchased from DBA Italia s.r.l. (Italy) and employed for the estimation of bulk molecular diffusion coefficients (see later on). Fourteen polystyrene standards (from Supelco SigmaAldrich, Milan, Italy) with molecular weights 500, 2000, 2500, 5000, 9000, 17 500, 30 000, 50 000, 156 000, 330 000, 565 000, 1 030 000, 1 570 000, and 2 310 000 were employed for inverse size exclusion chromatography (ISEC). The mobile phase (MP) was a binary mixture of hexane/ethanol (at different percentages).

2.2. Equipment

An UltiMate 3000 RS UHPLC chromatographic system from Thermo Fisher Dionex was used for the determination of van Deemter curves. This instrument consists of a dual gradient pump (flow rates up to 8.0 mL/min; pressure limit 800 bar under normal phase conditions), an in-line split loop well plate sampler, a thermostated column ventilated compartment and a diode array detector (UV Vanquish) with a low dispersion 2.5 μL flow cell. Detection wavelength was 214 nm (constant filter time: 0.002 s; data collection rate: 100 Hz; response time: 0.04 s). Two 350×0.10 mm I.D. Viper capillaries were used to connect the injector to the column and the column to the detector. The extra-column peak variance (calculated through peak moments) was 4.0 μL^2 at a flow rate of 1.0 mL/min. ISEC and peak parking experiments were carried out on an Agilent 1100 Series Capillary LC system equipped with a binary pump system, an autosampler, a column thermostat and a photodiode array detector.

2.3. Column and particle porosity

Porosities of each column were evaluated through Inverse Size Exclusion Chromatography (ISEC) [24]. 2 μL of polystirene standards dissolved in tetrahydrofuran were injected at a flow rate of 0.1 mL/min by using pure tetrahydrofuran as MP. Retention volumes were corrected for the extra-column contribution before being plotted against the cubic root of the molecular weight (M_w) [25]. The interstitial volume, V_e, was calculated by extrapolating to M_w=0 the excluded branch of this plot and the interstitial porosity of the column was calculated as:

$$\epsilon_e = V_e / V_{col} \tag{3}$$

being V_{col} the geometrical volume of the column. The thermodynamic void volume, V_0, was calculated from the corrected elution volume of benzene in tetrahydrofuran and it was used to estimate the total porosity:

$$\epsilon_t = V_0 / V_{col} \tag{4}$$

Particle porous zone porosity was, finally, calculated according to the following equation:

$$\epsilon_p = \frac{\epsilon_t - \epsilon_e}{(1-\epsilon_e)(1-\rho^3)} \tag{5}$$

with ρ being the core-to-particle diameter ratio ($\rho = 0$ for FPPs).

2.4. Estimation of diffusion coefficients

The peak parking method was used to estimate both effective, D_{eff}, and molecular, D_m, diffusion coefficients of TSO on the Whelk-O1 columns [26–28]. Measurements were performed at 35°C at four different hexane/ethanol MP compositions: 90:10, 95:5, 97:3 and 99:1 %(v/v). For the calculation of the spatial peak variance σ_x^2, the following equation was used:

$$\sigma_x^2 = \frac{L^2}{N} \tag{6}$$

where L is the column length and N is the number of theoretical plates. All the data were corrected for the extra-column peak variance. Parking times were 0, 120, 600, 1800 and 2400 s. The flow rate applied for the estimation of the effective diffusion coefficients was 0.3 mL/min.
Molecular diffusion coefficient of TSO in a variety of hexane/ethanol mixtures were measured by performing peak parking experiment in a column packed with non-porous particles (Micra column). Temperature was 35°C. In this case [16, 28]:

$$D_m = \frac{D_{eff}}{\gamma_e} \tag{7}$$

where γ_e is a geometrical parameter, called external obstruction factor, related to the tortuosity and constriction of inter-particle channels [29]. The value of γ_e was calculated by measuring D_{eff} (again by means of peak parking) for a molecule whose D_m is known from literature. To this purpose, thiourea in pure water at 25°C was used (D_m= 1.33×10^{-5} cm^2/s) [30]. γ_e was found to be 0.68. Calculated D_m for TSO under the different experimental conditions are reported under SI as well a thorough description of fundamental equations of mass transfer in chiral porous media.

2.5. van Deemter curve measurements

Van Deemter curves were recorded at 35°C by using hexane/ethanol 90:10 %(v/v) as mobile phase. Flow rates were changed from 0.1 mL/min up to 4.0 mL/min, with constant steps of 0.1 mL/min. Injection volume was 0.1 μL. Retention time and column efficiency (given as number of theoretical plates) of eluted peaks were automatically processed by the Chromeleon software (using peak width at half height, according to European Pharmacopeia) and corrected for the extra-column contribution.

3. Results and Discussion

Hereafter, the results derived by the application of these models will be employed to estimate of the different contributions to band broadening.
The characteristics of chiral particles studied in this work are listed in Table 1. Besides the information given by manufacturers, namely, particle diameter, pore size and specific surface area, both the bonding

density of chiral selector (calculated by elemental analysis) and the different porosities (total, particle porous-zone and interstitial) have been reported in the table. Bonding density of chiral selector has been expressed both as μmol per gram of bare silica and in μmol per square meter (specific bonding density).

Preparation of these CSPs is very reproducible, as reported in Refs. [2, 5, 31, 32]. A larger specific bonding density (+20% μmol/m^2) was systematically found on superficially-porous particles compared to fully-porous ones by taking experimental conditions constant during functionalization procedure. It is generally acknowledged that the larger the loading of chiral selector, the larger the enantioselectivity. This correlation has been usually explained by assuming a larger number of selective interactions on the CSPs where the surface amount of chiral selector is higher [33]. Nevertheless, some of the authors of this work found that instead of the number of sites, it is is rather the extent of binding that changes with the loading [23]. In general, however, little is known about the impact of the chiral selector loading on adsorption-desorption kinetics.

Regarding porosities, Table 1 reveals that for both columns the interstitial porosity, ϵ_e, is very close to the theoretical value typical of randomly packed beds of spherical particles (0.4). This is a rough confirmation that beds were densely packed [22]. The porous zone porosity, ϵ_p, is smaller on SPPs than on FPPs. Finally, the total porosity, ϵ_t, is smaller on the column made of SPPs than of FPPs, as a consequence of the unaccessible inner core present in the former.

To compare the performance of particles of different characteristics and dimensions, van Deemter curves have been expressed in reduced coordinates. Figure 1 shows the van Deemter curves of firstly and secondly-eluted enantiomers on the two columns employed in this work. In both cases, the MP was 90:10 %(v/v) hexane/ethanol mixture. A first interesting observation is that, at the optimum reduced velocity, the two enantiomers have very similar h (see Table 1 of SI). The longitudinal diffusion b is the dominant mechanism of mass transfer in this region. It can be rigorously estimated through stop-flow measurements (the so-called peak parking experiments), as described under the experimental section. Through these measurements, not only the effective diffusion coefficient of each enantiomer, $D_{eff,i}$ ($i = 1, 2$ respectively for the first and second enantiomer), but also their longitudinal diffusions (see eq. 5 of SI) can be derived:

$$b_i = 2(1 + k_{1,i})\frac{D_{eff,i}}{D_m} \qquad i = 1, 2 \tag{8}$$

In this equation, $k_{1,i}$ is the so-called "zone" retention factor of the i-th enantiomer, i.e., the retention factor based on the interstitial volume (eq. 9 of SI) [7, 34, 35]. Calculated b values are reported in Table 2. As expected, b is smaller on SPPs than on FPPs, due to the presence of the solid core that reduces the space available for diffusion in the former particles [36–38]. More interestingly it was found that, within experimental errors, b_1 and b_2 substantially coincide on each column, in agreement with the above observation about h at low flow velocities qualitatively made from Fig. 1.

From these findings, an interesting interpretation about the behavior of enantiomers in the adsorbed state can be derived. Let us start by assuming a model of diffusion in porous media. For the sake of simplicity, in this work the so-called parallel (or Knox) model will be employed [35]. This first-choice model assumes that all mass fluxes inside and outside the particle are additive. Therefore, $D_{eff,i}$ can be expressed as a time-average of the diffusion in the bulk MP, where the molecular diffusion coefficient is D_m, and of that in the porous zone, with molecular diffusion coefficient D_p, i.e. (see eq. 11 under SI):

$$D_{eff,i} = \frac{\gamma_e D_m + \frac{1-\epsilon_e}{\epsilon_e}(1 - \rho^3)D_{p,i}}{1 + k_{1,i}} \qquad i = 1, 2 \tag{9}$$

A schematic representation of the model under study is given in Figure 1 of SI. It is worth noticing that the only zone where chiral molecules are subjected to enantioselective interactions is on the particle surface, since no chiral additives were added to the MP. Accordingly, D_m is identical for the two enantiomers, while the porous zone molecular diffusion coefficient can be different ($D_{p,i},\ i = 1, 2$), as much as it also accounts for the contribution of surface diffusion. Indeed, by applying the parallel model of diffusion to the porous zone (in analogy with what was previously done with $D_{eff,i}$), $D_{p,i}$ can be expressed as the sum of diffusion in the stagnant MP contained in the pores (diffusion coefficient D_m) and surface diffusion (diffusion coefficient $D_{s,i},\ i = 1, 2$), see also Eq. 12 of SI [21, 39]:

$$D_{p,i} = \epsilon_p \gamma_p F(\lambda_m) D_m + (1 - \epsilon_p) K_{a,i} D_{s,i} \qquad i = 1, 2 \tag{10}$$

In this equation, γ_p is the internal obstruction factor (accounting for the tortuosity and the complex structure of mesopores), $F(\lambda_m)$ the hindrance diffusion factor describing the confinement of the sample within the narrow pores (of mesopore size λ_m) and $K_{a,i}$ is the Henry's adsorption constant (or distribution coefficient) of the i-th enantiomer. Enantioselectivity of the CSP follows from differences between $K_{a,1}$ and $K_{a,2}$ (see Table 1 under SI).
The introduction of Eqs. 10 and 9 in Eq. 8 leads to a complex expression for b_i, given as Eq. 13 of SI. However, by assuming $b_1 = b_2$ (see before) and by considering the physical properties of the system (Fig. 1 of SI), a very simple result is achieved (derivation of Eq. 11 is given under SI):

$$K_{a,1} \times D_{s,1} = K_{a,2} \times D_{s,2} \tag{11}$$

From Eq. 11, with $K_{a,1} \neq K_{a,2}$ (since the enantiomers are resolved on CSPs), it seems reasonable to get to the conclusion that:

$$D_{s,1} = D_{s,2} = 0 \tag{12}$$

or, said with different words, that the adsorption of both enantiomers is localized.
Indeed also:

$$K_{a,1}/K_{a,2} = D_{s,2}/D_{s,1} \tag{13}$$

is a solution of Eq. 11, for which however it is more difficult to provide a physically sound explanation.
In order to reinforce our hypothesis, a series of additional experiments were performed by changing the MP composition. The results of these experiments have been given in Table 2 of SI and graphically summarized in Fig. 2. As it can be noticed from this figure, the b coefficients of the two TSO enantiomers are, on both columns, always very close to each other (in the limit of experimental errors). Therefore, since different MP compositions lead to different values of equilibrium constant, the hypothesis $D_{s,1} = D_{s,2} = 0$ seems to be further strengthened.
On the other hand, the little differences observed in the longitudinal diffusion of the two enantiomers (on each column) may be explained by considering that, in the framework of this model, the surface diffusion coefficients are sort of lumped coefficients including the contributions of both selective and nonselective sites [23]. The excess isotherms [40] measured for hexane/ethanol binary mixtures on the Whelk-O1 CSPs represented in Fig. 3 show the preferential adsorption of ethanol on the stationary phase. Therefore, this suggests that surface diffusion should be limited also on nonselective sites due to the high viscosity of the layer of eluent adsorbed on the stationary phase [41].
This model would also explain the (relatively) larger differences observed in the b-terms measured on the column made of FPPs (compared to that of SPPs, see figure 2). This could be explained by considering the smaller bonding density of chiral selector on FPPs (see before) causing a larger contribution to retention and diffusion by nonselective interactions.
The other interesting observation from data in Fig. 2 (and from Table 2 of SI) is that the longitudinal diffusion is almost independent of the MP composition. This finding can be theoretically explained, firstly, by applying the condition $D_{s,1} = D_{s,2} = 0$ into Eq. 10 to calculate D_p. The calculated D_p is then introduced in Eq. 9. Finally, through Eq. 8 one arrives at:

$$b = 2\left[\gamma_e + \frac{1-\epsilon_e}{\epsilon_e}(1-\rho^3)\epsilon_p\gamma_p F(\lambda_m)\right] \tag{14}$$

Eq. 14 reveals that, when adsorption is localized, the longitudinal diffusion coefficient is independent from both the retention and the diffusion of a given analyte molecule, since the only contributions to b are geometrical factors.
By considering the solid liquid mass transfer resistance term c_s (calculated by means of eq. 10 of SI), our results show that it is smaller on SPPs than on FPPs independently from MP composition. This is in agreement with the reduced intraparticle space available for diffusion on the former type of particles [36–38] (see Tables 2 for 90:10 and 2 of SI for other MP compositions). Moreover, it is interesting to notice that, for a given MP composition, c_s increases with increasing retention. Indeed it is larger for the most retained enantiomer than for the less retained one. This is the opposite of what happens in RPLC, where the larger the retention the smaller c_s. This apparent contradiction can be explained again by considering that solid phase diffusion is negligible in the system under investigation. On the opposite, solid phase diffusion is the most important mechanism of mass transfer through pores in RPLC [1, 32]. Eq. 20 of SI shows that, if the adsorption is localized, c_s does indeed not depend on diffusion.
In the second part of this study, we will focus on the combined contribution to band broadening by adsorption-desorption kinetics and eddy dispersion at 90:10% (v/v) hexane/ethanol. By looking again

at Fig. 1, it can be observed that van Deemter curves of first enantiomers on the two columns consistently lay below those of the second ones and that the gap between the curves of the two enantiomers is more pronounced on the SPPs column than on the FPPs one. This gap cannot be explained only in terms of c_s (see Table 2). As it usually happens in chiral chromatography, the contribution of the slow adsorption-desorption kinetics cannot be neglected.

As it was pointed out before, however, the term c_{ads} cannot be directly estimated through the subtraction method, which would lead to Eq. 2. In order get an estimation of the relative importance of these two terms, the study of adsorption equilibria can help. The adsorption binding constants (determined, e.g., through adsorption isotherms) are indeed correlated to the adsorption-desorption kinetics [1, 7, 42]. In a previous work, some of the authors of this paper measured the adsorption isotherms of TSO enantiomers on the same Whelk-O1 CSPs and under the same experimental conditions [23]. It was found that the binding constants were systematically higher on the SPPs than on the FPPs. This finding was likely correlated to the higher specific loading of chiral selector of SPPs (see Table 1).

In Fig. 4 the study of how the combined contribution of c_{ads} and $a(\nu)$ changes with ν is reported for the second eluted TSO enantiomer on the two Whelk-O1 columns. From this plot two considerations can be made: i) the sum of c_{ads} and $a(\nu)$ is consistently higher on the 2.6 μm SPPs column than on the fully porous one; ii) since at small interstitial velocities the term $c_{ads}\nu$ is negligible, it is reasonable to hypothesize that, in this region, the contribution of eddy dispersion is higher on the SPP column compared to the FPP one. These results are in agreement with previous findings on the same columns. Essentially the higher eddy dispersion could be due to the difficulties encountered during packing procedure of chiral SPPs. Indeed, not only the achievement of stable slurry suspensions was more difficult with Whelk-O1 SPPs than with their fully porous counterparts but also, for instance, the time needed to compress the bed did not follow any expected trend nor could be optimized. This issues were not observed with Whelk-O1 FPPs [1, 7]. Moreover, the two curves do not tend towards zero for the smallest ν value, indicating that border effects cannot be fully concealed due to a slow radial equilibration across the column diameter on both columns (the same happens, e.g., in HILIC mode [43]).

4. Conclusions

The study of mass transfer phenomena in chiral chromatography is complicated by the intrinsic difficulty of directly estimating the adsorption-desorption kinetics. In this work, the combination of kinetic and thermodynamic measurements has allowed to shed some light on the nature of both surface diffusion and adsorption-desorption kinetics on Pirkle-type Whelk-O1 CSPs. The application of the parallel model of diffusion and the estimation of excess isotherms has allowed to point out that in NP conditions the surface diffusion of enantiomers is negligible, leading to the independence of the longitudinal diffusion coefficient from both retention and diffusion. Even though this could be somehow expected under normal phase conditions, for which retention has always been considered to be adsorption-driven and no surface diffusion has been thought to occur – see, e.g., references [39, 44, 45] for achiral separations – to the best of our knowledge this is the first time where this has been experimentally proved.

Results of this work also confirmed the importance of adsorption-desorption kinetics on efficiency in chiral separations. This is a very important point to further improve the design of more efficient columns in the future. However, some points are still open. Firstly, it will be very important to understand how c_{ads} depends on some experimental variables such as the mobile phase composition, the temperature and the chiral selector loading. Another fundamental point is to find a correlation between kinetic and thermodynamic parameters by combining mass transfer investigation and adsorption isotherm determination.

5. Acknowledgements

The authors thank the Italian University and Scientific Research Ministry (Grant PRIN 2017Y2PAB8_003) and the Laboratory Terra&Acqua Tech, member of Energy and Environment Cluster, Technopole of Ferrara of Emilia-Romagna High Technology Network. Dr. M. Carmosino from the University of Ferrara is acknowledged for technical support.

6. Figures

Figure captions

Figure 1. Reduced van Deemter curves of: (i) first (squares) and second (circles) eluted TSO enantiomers on the 2.5 μm FPP (box a) and the 2.6 μm SPP (box b) Whelk-O1 columns, measured at 90:10 % (v/v) hexane/ethanol.

Figure 2. Dependence of the reduced longitudinal diffusion term, b, of TSO enantiomers on MP composition expressed as percentage of ethanol for 2.6 μm SPP (blue squares) and 2.5 μm FPP (red points) Whelk-O1 columns.

Figure 3. Excess adsorption isotherms on the 2.6 μm SPP (green) and 2.5 μm FPP (blue) columns expressed as excess volume of ethanol adsorbed on the stationary phase (V^{exc}_{EtOH}) as a function of the volume fraction of EtOH (θ^m EtOH) in the MP. Modified with permission from [23].

Figure 4. Dependence of $a(\nu) + c_{ads}\nu$ on ν for 2.6 μm SPP (blue squares) and the 2.5 μm FPP (red circles) Whelk-O1 columns, measured at 90:10 % (v/v) hexane/ethanol.

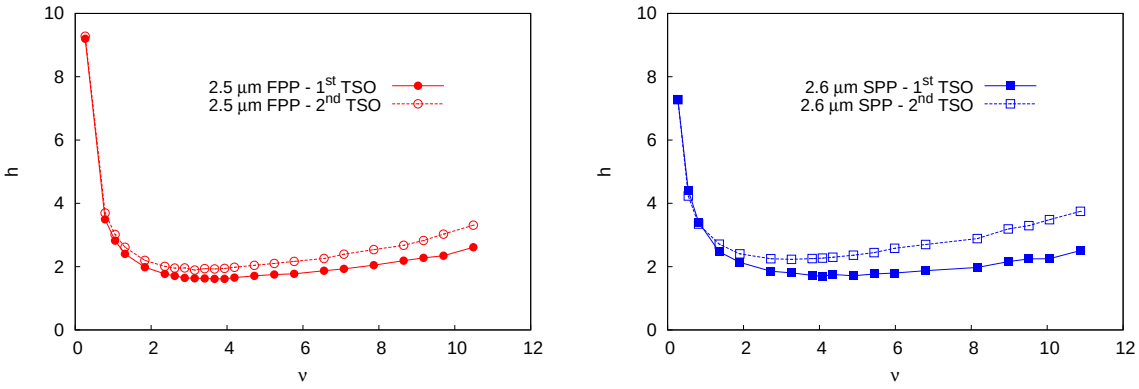

(a) (b)

Figure 1

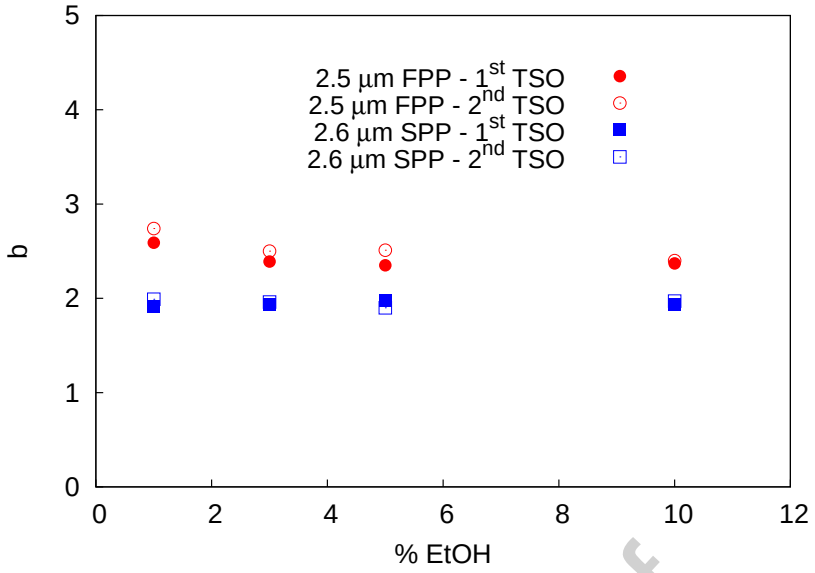

Figure 2

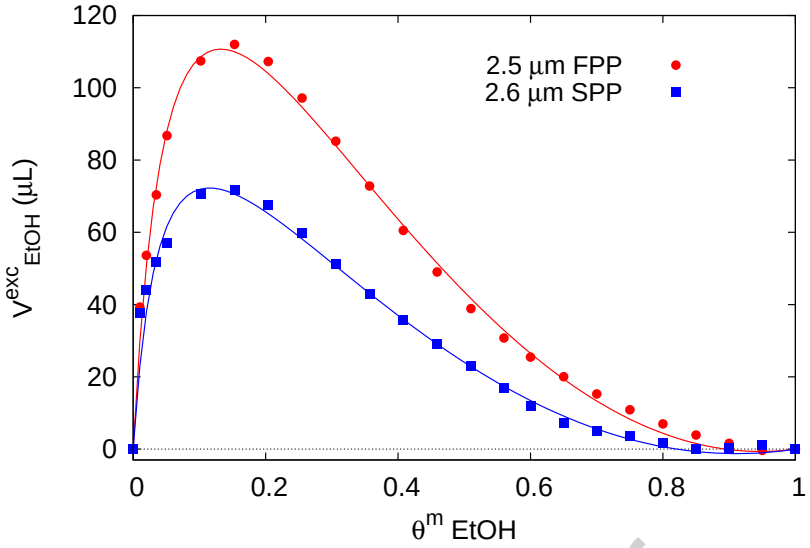

Figure 3

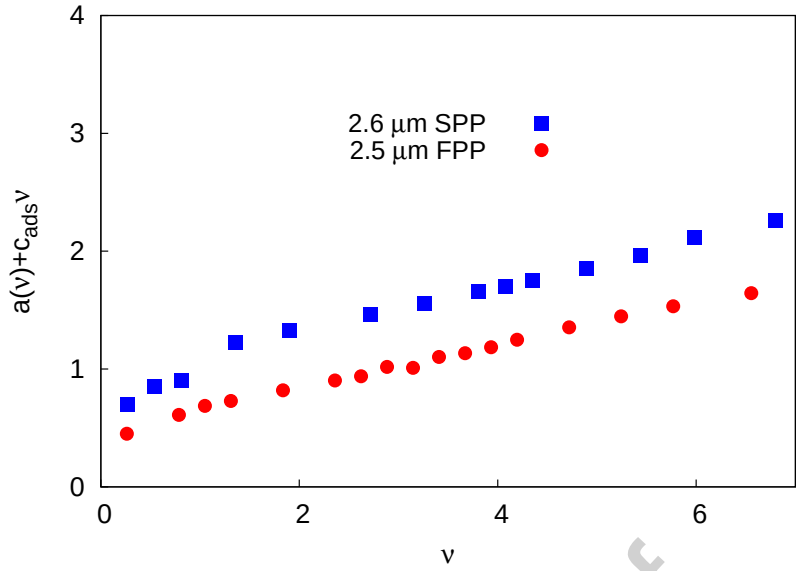

Figure 4

7. Tables

Table 1: Geometrical and physico-chemical characteristics of Whelk-O1 chiral particles and columns. Brand: commercial silica name; particle type: FPP = fully porous, SPP = superficially porous; d_p: particle diameter; A_s: specific surface area; ϵ_t: total porosity; ϵ_e: external porosity; ϵ_p: particle porous zone porosity.

Brand /Particle type	d_p μm	A_s m^2/g	Pore size Å	Bonding density μmol/g	μmol/m^2	ϵ_t	ϵ_e	ϵ_p
Kromasil /FPP	2.5	323	100	391	1.2	0.67	0.41	0.44
Accucore /SPP	2.6	130	80	190	1.5	0.52	0.41	0.25

Table 2: Zone retention factor (k_1), effective diffusion coefficient (D_{eff}), reduced longitudinal diffusion coefficient (b), reduced solid-liquid mass transfer resistance coefficient (c_s), particle diffusivity (D_p)measured on the Whelk-O1 chiral particles.

Column	k_1		$D_{eff} \times 10^{-6}$ (cm^2/s)		b		c_s		$D_p \times 10^{-6}$ (cm^2/s)	
	1^{st}	2^{nd}	1^{st}	2^{nd}	1^{st}	2^{nd}	1^{st}	2^{nd}	1^{st}	2^{nd}
2.5μm FPP	1.9	3.7	9.6	5.9	2.4	2.4	0.026	0.037	8.8	8.8
2.6μm SPP	1.2	2.4	11.0	6.8	2.0	2.0	0.015	0.022	7.2	7.2

References

[1] O. H. Ismail, L. Pasti, A. Ciogli, C. Villani, J. Kocergin, S. Anderson, F. Gasparrini, A. Cavazzini, M. Catani, Pirkle-type chiral stationary phase on coreshell and fully porous particles: Are superficially porous particles always the better choice toward ultrafast high-performance enantioseparations?, J. Chromatogr. A 1466 (2016) 96–104.

[2] O. H. Ismail, A. Ciogli, C. Villani, M. D. Martino, M. Pierini, A. Cavazzini, D. S. Bell, F. Gasparrini, Ultra-fast high-efficiency enantioseparations by means of a teicoplanin-based chiral stationary phase made on sub-2 μm totally porous silica particles of narrow size distribution, J. Chromatogr. A 1427 (2016) 55–68.

[3] D. C. Patel, Z. S. Breitbach, J. Yu, K. A. Nguyen, D. W. Armstrong, Quinine bonded to superficially porous particles for high-efficiency and ultrafast liquid and supercritical fluid chromatography, Anal. Chim. Acta 963 (2017) 164–174.

[4] Q. Kharaishvili, G. Jibuti, T. Farkas, B. Chankvetadze, Further proof to the utility of polysaccharide-based chiral selectors in combination with superficially porous silica particles as effective chiral stationary phases for separation of enantiomers in high-performance liquid chromatography, J. Chromatogr. A 1467 (2016) 163–168.

[5] O. H. Ismail, M. Antonelli, A. Ciogli, C. Villani, A. Cavazzini, M. Catani, S. Felletti, D. S. Bell, F. Gasparrini, Future perspectives in high efficient and ultrafast chiral liquid chromatography through zwitterionic teicoplanin-based 2μm superficially porous particles, J. Chromatogr. A 1520 (2017) 91–102.

[6] D. C. Patel, Z. S. Breitbach, M. F. Wahab, C. L. Barhate, D. W. Armstrong, Gone in seconds: praxis, performance and peculiarities of ultrafast chiral liquid chromatography with superficially porous particles, Anal. Chem. 87 (2015) 9137–9148.

[7] M. Catani, O. H. Ismail, F. Gasparrini, M. Antonelli, L. Pasti, N. Marchetti, S. Felletti, A. Cavazzini, Recent advancements and future directions of superficially porous chiral stationary phases for ultrafast high-performance enantioseparations, Analyst 142 (2017) 555–566.

[8] R. M. Wimalasinghe, C. A. Weatherly, Z. S. Breitbach, D. W. Armstrong, Hydroxypropyl beta cyclodextrin bonded superficially porous particlebased HILIC stationary phases, J. Liq. Chromatogr. Rel. Tech. 39 (2016) 459–464.

[9] D. C. patel, M. F. Wahab, D. W. Armstrong, Z. S. Breitbach, Salient sub-second separations, Anal. Chem. 88 (2016) 8821–8826.

[10] O. H. Ismail, G. L. Losacco, G. Mazzoccanrti, A. Ciogli, C. Villani, M. Catani, L. Pasti, S. Anderson, A. Cavazzini, F. Gasparrini, Unmatched kinetic performance in enantioselective supercritical fluid chromatography by combining latest generation Whelk-O1 chiral stationary phases with a low-dispersion in-house modified equipment, Anal. Chem. 90 (2018) 10828–10836.

[11] O. H. Ismail, S. Felletti, C. D. Luca, L. Pastia, N. Marchetti, V. Costa, F. Gasparrini, A. Cavazzini, M. Catani, The way to ultrafast, high-throughput enantioseparations of bioactive compounds in liquid and supercritical fluid chromatography, Molecules 23 (2018) 2709.

[12] C. L. Barhate, Z. S. Breitbach, E. C. Pinto, E. L. Regalado, C. J. Welch, D. W. Armstrong, Ultrafast separation of fluorinated and desfluorinated pharmaceuticals using highly efficient and selective chiral selectors bonded to superficially porous particles, J. Chromatogr. A 1426 (2015) 241–247.

[13] F. Gritti, G. Guiochon, Mass transfer mechanism in chiral reversed phase liquid chromatography, J. Chromatogr. A 1332 (2014) 35–45.

[14] L. D. Asnin, A. A. Boteva, O. P. Krasnykh, M. V. Stepanova, I. Ali, Unusual van deemter plots of optical isomers on a chiral brush-type liquid chromatography column, J. Chromatogr. A 1592 (2019) 112–121.

[15] L. Pasti, N. Marchetti, R. Guzzinati, M. Catani, V. Bosi, F. Dondi, A. Sepsey, A. Felinger, A. Cavazzini, Microscopic models of liquid chromatography: From ensemble-averaged information to resolution of fundamental viewpoint at single-molecule level, TrAC 81 (2016) 63–68.

[16] F. Gritti, G. Guiochon, Mass transfer kinetics, band broadening and column efficiency, J. Chromatogr. A 1221 (2012) 2–40.

[17] M. Catani, S. Felletti, O. H. Ismail, F. Gasparrini, L. Pasti, N. Marchetti, C. D. Luca, V. Costa, A. Cavazzini, New frontiers and cutting edge applications in ultra high performance liquid chromatography through latest generation superficially porous particles with particular emphasis to the field of chiral separations, Anal. Bioanal. Chem 410 (2018) 2457–2465.

[18] S. Felletti, C. D. Luca, G. Lievore, T. Chenet, B. Chankvetadze, T. Farkas, A. Cavazzini, Shedding light on mechanisms leading to convex-upward van deemter curves on a cellulose tris(4-chloro-3-methylphenylcarbamate)-based chiral stationary phase, J. Chromatogr. A 1630 (2020) 461532.

[19] K. Schmitt, U. Woiwode, M. Kohout, T. Zhang, W. Lindner, M. Lämmerhofer, Comparison of small size fully porous particles and superficially porous particles of chiral anion-exchange type stationary phases in ultra-high performance liquid chromatography: effect of particle and pore size on chromatographic efficiency and kinetic performance, J. Chromatogr. A 1569 (2018) 149–159.

[20] C. Geibel, K. Dittrich, U. Woiwode, M. Kohout, T. Zhang, W. Lindner, M. Lämmerhofer, Evaluation of superficially porous particle based zwitterionic chiralion exchangers against fully porous particle benchmarks forenantioselective ultra-high performance liquid chromatography, J. Chromatogr. A 1603 (2019) 130–140.

[21] G. Guiochon, A. Felinger, A. Katti, D. Shirazi, Fundamentals of Preparative and Nonlinear Chromatography, 2nd Edition, Academic Press, Boston, MA, 2006.

[22] G. Desmet, S. Deridder, Effective medium theory expressions for the effective diffusion in chromatographic beds filled with porous, non-porous and porous-shell particles and cylinders. Part I: Theory, J. Chromatogr. A 1218 (2011) 32–45.

[23] S. Felletti, C. De Luca, O. H. Ismail, L. Pasti, V. Costa, F. Gasparrini, A. Cavazzini, M. Catani, On the effect of chiral selector loading and mobile phase composition on adsorption properties of latest generation fully- and superficially-porous whelk-o1 particles for high-efficient ultrafast enantioseparations, J. Chromatogr. A 1579 (2018) 41–48.

[24] I. Halász, K. Martin, Pore Size of Solids, Angew. Chem. Int. Ed. Engl 17 (1978) 901–908.

[25] A. Cavazzini, F. Gritti, K. Kaczmarski, N. Marchetti, G. Guiochon, Mass-transfer kinetics in a shell packing materials for chromatography, Anal. Chem. 79 (2007) 5972–5979.

[26] F. Gritti, G. Guiochon, Theoretical and experimental impact of the bed aspect ratio on the axial dispersion coefficient of columns packed with 2.5μm particles, J. Chromatogr. A 1262 (2012) 107–121.

[27] J. H. Knox, L. McLaren, New gas chromatographic method for measuring gaseous diffusion coefficients and obstructive factors, Anal. Chem. 36 (1964) 1477–1482.

[28] K. Miyabe, Y. Matsumoto, G. Guiochon, Peak parking-moment analysis. A strategy for the study of the mass-transfer kinetics in the stationary phase, Anal. Chem. 79 (2007) 1970–1982.

[29] J. C. Giddings, Comparison of theoretical limit of separating speed in gas and liquid chromatography, Anal. Chem. 37 (1965) 60–63.

[30] D. Ludlum, R. Warner, H. Smith, The Diffusion of thiourea in water at 25°C, J. Phys. Chem 66 (1962) 1540–1542.
[31] O. H. Ismail, M. Catani, L. Pasti, A. Cavazzini, A. Ciogli, C. Villani, D. Kotoni, F. Gasparrini, D. S. Bell, Experimental evidence of the kinetic performance achievable with columns packed with the new 1.9 μm fully porous particles Titan c_{18}, J. Chromatogr. A 1454 (2016) 86–92.
[32] M. Catani, O. H. Ismail, A. Cavazzini, A. Ciogli, C. Villani, L. Pasti, D. Cabooter, G. Desmet, F. Gasparrini, D. S. Bell, Rationale behind the optimum efficiency of columns packed with the new 1.9 μm fully porous particles titan C_{18}, J. Chromatogr. A 1454 (2016) 78–85.
[33] A. Cavazzini, L. Pasti, A. Massi, N. Marchetti, F. Dondi, Recent applications in chiral high performance liquid chromatography: A review, Anal. Chim. Acta 706 (2011) 205–222.
[34] G. Desmet, K. Broeckhoven, J. D. Smet, S. Deridder, G. V. Baron, P. Gzil, Errors involved in the existing B-term expressions for the longitudinal diffusion in fully porous chromatographic media. part I: Computational data in ordered pillar arrays and effective medium theory, J. Chromatogr. A 1188 (2008) 171–188.
[35] J. H. Knox, H. P. Scott, B and C terms in the van Deemter equation for liquid chromatography, J. Chromatogr. 282 (1983) 297–313.
[36] G. Guiochon, F. Gritti, Shell particles, trials, tribulations and triumphs, J. Chromatogr. A 1218 (2011) 1915–1938.
[37] A. Cavazzini, F. Gritti, K. Kaczmarski, N. Marchetti, G. Guiochon, Mass-transfer kinetics in a shell packing material for chromatography, Anal. Chem. 79 (2007) 5972–5979.
[38] S. Deridder, M. Catani, A. Cavazzini, G. Desmet, A theorethical study on the advantage of core-shell particles with radially-oriented mesopores, J. Chromatogr. A 1456 (2016) 137–144.
[39] K. Miyabe, G. Guiochon, Surface diffusion in reversed-phase liquid chromatography, J. Chromatogr. A 1217 (2010) 1713–1734.
[40] F. Chan, L. S. Yeung, R. LoBrutto, Y. V. Kazakevich, Interpretation of the excess adsorption isotherms of organic eluent components on the surface of reversed-phase phenyl modified adsorbents, J. Chromatogr. A 1082 (2005) 158–165.
[41] C. Zhao, N. M. Cann, Solvation of the Whelk-O1 chiral stationary phase: A molecular dynamics study, J. Chromatogr. A 1131 (2006) 110–129.
[42] G. Guiochon, A. Felinger, D. G. Shirazi, A. Katti, Fundamentals of preparative and nonlinear chromatography, 2nd Edition, Elsevier Academic Press, Amsterdam, 2006.
[43] G. Gritti, G. Guiochon, Mass transfer mechanism in hydrophilic interaction chromatography, J. Chromatogr. A 1302 (2013) 55–64.
[44] F. Gritti, G. Guiochon, Mass transfer kinetics, band broadening and column efficiency, J. Chromatogr. A 1221 (2012) 2–40.
[45] P. Jandera, T. Hájek, Mobile phase effects on the retention on polar columns with special attention to the dual hydrophilic interactionreversedphase liquid chromatography mechanism, a review, J. Sep. Sci. 41 (2018) 145–152.

Declaration of Competing Interest

The authors declare that they have no known competing financial interests or personal relationships that could have appeared to influence the work reported in this paper.

AUTHORS CONTRIBUTIONS

Simona Felletti: Investigation, Software, Formal Analysis, Methodology, Writing Original Draft
Martina Catani: Investigation, Methodology, Conceptualization, Writing - Review & Editing
Giulia Mazzoccanti: Investigation, Validation
Chiara De Luca: Investigation, Validation
Giulio Lievore: Data Curation
Alessandro Buratti: Data Curation
Luisa Pasti: Formal Analysis
Francesco Gasparrini: Supervision, Resources, Project administration, Writing - Review & Editing
Alberto Cavazzini: Supervision, Funding Acquisition, Project administration, Resources, Conceptualization, Writing - Review & Editing